Utility of ^{18}F-FDG PET/CT Uptake Patterns in Waldeyer's Ring for Differentiating Benign from Malignant Lesions in Lateral Pharyngeal Recess of Nasopharynx

Yen-Kung Chen[1], Chen-Tau Su[2], Kwan-Hwa Chi[3], Ru-Hwa Cheng[1], Su-Chen Wang[1], and Chung-Huei Hsu[4]

[1]Department of Nuclear Medicine, Shin Kong Wu Ho-Su Memorial Hospital, School of Medicine, Taipei Medical University and Fu Jen Catholic University, Taipei, Taiwan; [2]Department of Medical Imaging, Shin Kong Wu Ho-Su Memorial Hospital, Taipei, Taiwan; [3]Department of Radiation Therapy and Oncology, Shin Kong Wu Ho-Su Memorial Hospital, Taipei, Taiwan; [4]Department of Nuclear Medicine, Taipei Medical University Hospital, Taipei, Taiwan

Focally increased ^{18}F-FDG uptake in the lateral pharyngeal recess (LPR) of the nasopharynx due to a benign or malignant lesion is not an uncommon finding on PET images. The aim of this study was to evaluate whether, on PET/CT images, ^{18}F-FDG uptake occurs with characteristic patterns and intensities in various regions of Waldeyer's ring that can improve our ability to differentiate benign from malignant lesions. **Methods:** Data generated from the ^{18}F-FDG PET/CT images of 1,628 subjects in our cancer-screening program were analyzed. Increased uptake in the LPR was observed in 80 subjects (4.9%) presenting with benign lesions, including 53 subjects without and 27 subjects with symptoms of upper airway discomfort. In addition, 30 healthy controls and 21 patients with newly diagnosed nasopharyngeal carcinoma were recruited for this study. Visual uptake, measurements of the lesions' standardized uptake value (SUV), and any abnormalities on PET/CT were evaluated. The receiver-operating-characteristic curve and area under the curve were applied to evaluate the discriminating power. **Results:** Increased ^{18}F-FDG uptake (SUV, mean ± SD) was found in the LPR, with a statistically significant ($P < 0.001$) difference between benign lesions (3.0 ± 1.16) and malignant lesions (7.03 ± 3.83). However, associated increased uptake exclusively in the palatine tonsil, lingual tonsil, and submandibular gland was found in both asymptomatic and symptomatic subjects. The ratio of LPR uptake to palatine tonsil uptake (N/P ratio) in benign lesions (0.81 ± 0.37) was significantly ($P < 0.001$) lower than that in malignant lesions (2.30 ± 1.62). Higher incidences of asymmetric ^{18}F-FDG LPR uptake, cervical lymph node uptake, and asymmetric wall thickening of the LPR on CT were observed in patients with nasopharyngeal carcinoma. When an SUV of less than 3.9 and an N/P ratio of less than 1.5 were used as cutoff points in subjects showing the combination of symmetric uptake in the LPR and normal or symmetric wall thickening, and detectable lymph node uptake, the area under the curve for benign lesions on PET/CT was 0.932 ± 0.042 (95% confidence interval, 0.86–0.98), with a sensitivity of 90.4% and a specificity of 93.8%. **Conclusion:** The intensity and patterns of ^{18}F-FDG uptake in various regions of Waldeyer's ring along with CT scan findings provide a feasible modality to differentiate benign from malignant nasopharyngeal lesions.

Key Words: PET/CT; nasopharyngeal carcinoma; Waldeyer's ring

Nasopharyngeal carcinoma (NPC) is an epithelial malignancy occurring worldwide, with a particularly high prevalence in southern China, Hong Kong, Singapore, and Taiwan (*1–3*). It is now believed that inflammation and other benign conditions predispose the nasopharyngeal mucosa to undergo transformation associated with an increased risk of malignancy. Epstein-Barr virus is a ubiquitous human herpesvirus infecting over 90% of the adult population worldwide. Primary infection with Epstein-Barr virus usually occurs early in life and is asymptomatic. In any case, primary infection is followed by lifelong viral persistence, which again is asymptomatic in most cases (*4–6*). Small tumors in the nasopharynx seldom result in symptoms, and with these tumors being clinically inaccessible, a prompt diagnosis is difficult. In addition, primary malignancies of the nasopharynx are often understaged by conventional examinations. Patients with squamous cell carcinoma of the head and neck sometimes present solely with metastatic cervical nodes without an identifiable primary site.

^{18}F-FDG PET can detect unknown primary tumors in 30%–50% of patients with metastatic cervical lymph nodes without a clinically detectable primary tumor (*7*). Unfortunately, false-positive results are possible with ^{18}F-FDG PET alone, because an infectious or inflammatory process producing uptake might be present, and because physiologic uptake into structures such as tonsils, salivary glands, and

muscles might occur (*8,9*). To accurately interpret PET images of the head and neck, one must be fully familiar with the variable patterns and intensities of uptake and with the frequencies of physiologic uptake. Images obtained with a combined PET/CT scanner depict exact anatomic landmarks, enable precise localization of metabolic abnormalities, and correctly identify physiologic, nonspecific uptake that would otherwise be mistaken for a malignant tumor. The aim of this study was to evaluate whether, on PET/CT images, ^{18}F-FDG uptake occurs with characteristic patterns and intensities in various regions of Waldeyer's ring that can improve our ability to differentiate benign from malignant lesions.

MATERIALS AND METHODS

Subjects

A prospective study was designed. From March 2004 to March 2005, 1,628 subjects (840 male and 788 female; mean age ± SD, 52.4 ± 12.7 y) were enrolled in our ^{18}F-FDG PET/CT cancer-screening program. Among them, 80 subjects (4.9%) had focally increased ^{18}F-FDG uptake, defined as an uptake intensity greater than physiologic liver uptake, in the lateral pharyngeal recess (LPR) of the nasopharynx. They were identified as having benign lesions and were subdivided into a group that had symptoms in the upper respiratory airway (27 subjects [1.7%]; 18 male and 9 female; mean age, 43.4 ± 9.2 y) and an asymptomatic group without a related specific medical history (53 subjects [3.3%]; 22 male and 31 female; mean age, 48.7 ± 10.9 y). In addition, we recruited a healthy control group consisting of 30 subjects (12 male and 18 female; mean age, 51.9 ± 9.6 y) in this cancer-screening program without any symptom or sign related to recent or chronic discomfort of the ear, nose, or throat region and with no or only faintly visible ^{18}F-FDG uptake in the LPR of the nasopharynx. The above classifications were correlated with the initial clinical evaluation, histologic findings (1 in the symptomatic group and 7 in the asymptomatic group), endoscopic findings (1 in the symptomatic group and 9 in the asymptomatic group), and imaging findings (contrast-enhanced CT and MRI). A long-term clinical follow-up period of at least 1 y was mandatory to reach the conclusion. Retrospectively, 21 patients (16 male and 5 female; mean age, 48.1 ± 14.9 y) with histologically proven newly diagnosed NPC referred by clinical physicians for initial staging were also recruited in this study. Most of the patients with NPC were included in our previous report (*10*).

Three subjects (10%) in the control group, 3 (11%) in the symptomatic group, 5 (1%) in the asymptomatic group, and 8 (38%) in the NPC group were cigarette smokers. All subjects gave informed consent to participate in this study according to the guidelines established by the local ethics committee and the Helsinki Declaration.

^{18}F-FDG PET Imaging Protocol

All patients were imaged with a PET/CT system (Discovery LS; GE Healthcare). The patients were required to fast for at least 8 h before the PET/CT scan but had to be well hydrated and not have engaged in strenuous work or exercise for 24 h before the scan. As many sequential images as necessary to include the entire head, thorax, abdomen, and pelvis were obtained. In the PET/CT scanner, the PET attenuation correction factors were calculated from the CT images. CT was performed using a 4-detector-row spiral CT scanner (LightSpeed; GE Healthcare). Acquisitions occurred at 5–7 bed positions under the following parameters: 140 kV, 40 mA, 0.8 s per CT rotation, a pitch of 6, a table speed of 22.5 mm/s, coverage of 722.5–1,011.5 mm, and an acquisition time of 31.9–37 s. CT was performed before the emission acquisition. CT data were resized from a 512 × 512 matrix to a 128 × 128 matrix to match the PET data so that the images could be fused and CT transmission maps generated. The transaxial resolution (full width at half maximum) of PET/CT was 4.8 mm. After intravenous administration of 370 MBq (10 mCi) of ^{18}F-FDG, emission images were acquired for 5 min per bed position. The uptake period between the ^{18}F-FDG injection and the beginning of the emission scan was 60 ± 10 min (range, 50–70 min). Image datasets were obtained by iterative reconstruction (using ordered-subset expectation maximization). Images were displayed in 3 orthogonal projections and as whole-body maximum-pixel-intensity reprojections for visual interpretation. A workstation (Xeleris; GE Healthcare) was used for image display and analysis.

Image Interpretation

The images were jointly interpreted by 2 experienced physicians working in consensus: one from the Department of Diagnostic Radiology and the other from the Department of Nuclear Medicine. They were aware of the subjects' clinical history, as provided by the referring physicians, but were unaware of the results of other, if any, imaging studies performed. Initially, the attenuation-corrected PET images were reviewed as maximum intensity projections and in transaxial, coronal, and sagittal planes. The locations of lesions showing abnormal ^{18}F-FDG uptake were subsequently correlated with the PET/CT findings. In addition, the images were semiquantitatively analyzed by measuring the mean standardized uptake values (SUVs) bilaterally in the LPR regions of the nasopharynx, soft palate, lymphoid tissue in Waldeyer's ring (including the palatine and lingual tonsils), and salivary glands (including the parotid, submandibular, and sublingual glands). For the measurements, the region of interest was placed on the transaxial plane of the emission image with an ^{18}F-FDG uptake area 1 cm in diameter. The SUV was calculated as (activity in the region of interest [MBq/mL])/(injected dose [MBq]/patient's weight [kg]). ^{18}F-FDG uptake differing by more than 1.0 between the sides was considered to be asymmetric uptake. Wall thickening of the LPR was considered to be present when the CT images showed obliteration of the Rosenmüller fossa and increased soft-tissue density.

Data and Statistical Analyses

Statistical analyses were performed for each region of the studied group by computing the mean ± SD of the SUV. Differences were compared using 1-way ANOVA followed by the Student *t* test for unpaired data. In addition, the χ^2 test was used for comparing differences in PET/CT parameters between benign and malignant lesions. A value of *P* less than 0.05 was considered to indicate a statistically significant difference. Receiver-operating-characteristic curves and calculation of the area under the curve (AUC) were applied to evaluate the efficacy of the imaging methods.

RESULTS

Example ^{18}F-FDG PET/CT images of the nasopharynx region are presented in Figure 1. Increased ^{18}F-FDG uptake in the adult adenoid and musculus longus capitis was
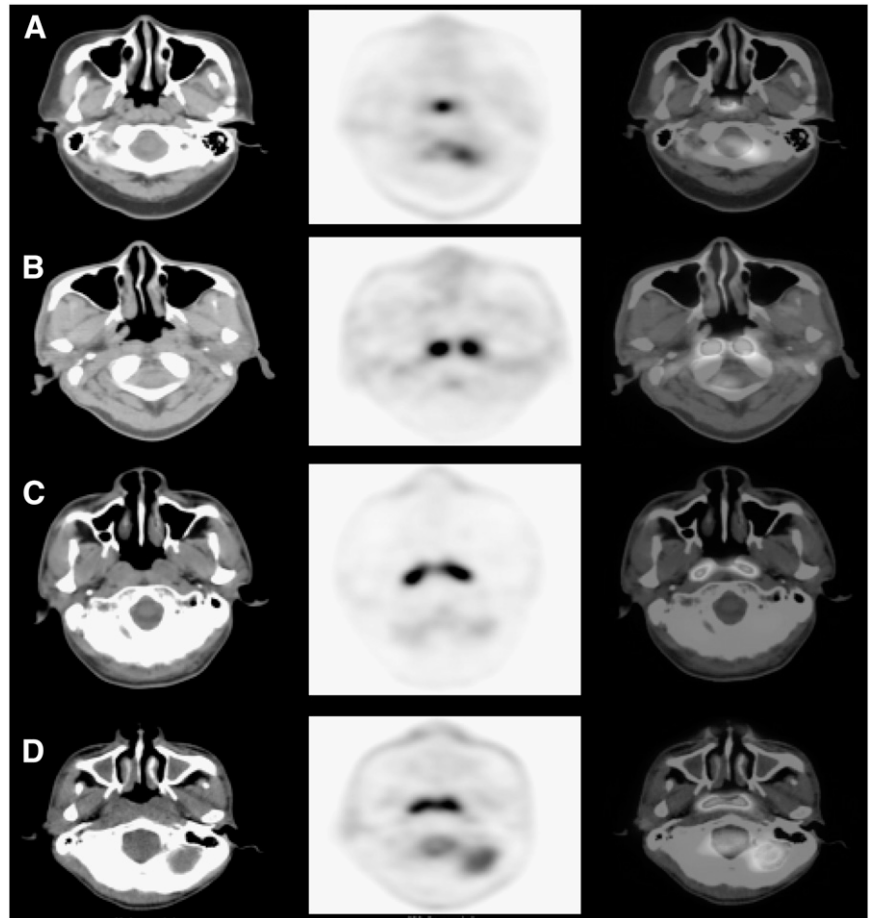
FIGURE 1. CT (left), PET (middle), and fused PET/CT (right) images of nasopharynx in 3 asymptomatic subjects (A–C) and 1 symptomatic subject (D): nasopharyngeal adenoid hypertrophy with ^{18}F-FDG uptake (A), longus capitis muscle with ^{18}F-FDG uptake (B), symmetric ^{18}F-FDG uptake in LPR of nasopharynx (C), and symmetric ^{18}F-FDG uptake and wall thickening in LPR of nasopharynx (D).

seldom obvious, and wall thickening of the LPR could not be assessed using PET. The exact locations and morphologic changes of the lesions had to be interpreted using coregistered CT.

Table 1 shows the SUVs (mean $\pm$ SD) of various regions of Waldeyer's ring and the salivary glands for the healthy, asymptomatic, symptomatic, and NPC groups. Among the 30 healthy controls, no or only mild ^{18}F-FDG uptake, with an SUV of 1.36 ± 0.28, was observed in the LPR. The palatine tonsil usually showed mildly increased ^{18}F-FDG uptake, with an SUV of 3.22 ± 0.71. The asymptomatic group showed significantly increased ^{18}F-FDG uptake in the LPR (2.90 ± 1.02, $P < 0.001$), palatine tonsil (3.97 ± 1.54, $P = 0.007$), lingual tonsil (2.58 ± 0.85, $P = 0.023$), and submandibular gland (1.68 ± 0.48, $P = 0.007$). The symptomatic group revealed significantly increased ^{18}F-FDG uptake in the LPR (3.18 ± 1.38, $P < 0.001$), palatine tonsil (3.97 ± 1.58, $P = 0.015$), lingual tonsil (2.89 ± 1.08, $P = 0.004$), and submandibular gland (1.65 ± 0.47, $P = 0.027$) as well. There was no statistical difference in any region of Waldeyer's ring or the salivary glands between the asymptomatic group and the symptomatic group. Patients with NPC had intense ^{18}F-FDG uptake in the LPR (7.03 ± 3.83), with significantly increased SUVs when compared with the healthy group ($P < 0.001$). Otherwise, no significant SUV difference was observed in any region of Waldeyer's ring or the salivary glands when patients with NPC were compared with the healthy group. Additionally, lower SUVs were found in the palatine tonsil, lingual tonsil, and submandibular gland when patients with NPC were compared with either the asymptomatic group ($P = 0.013$, 0.044, and 0.008, respectively) or the symptomatic group ($P = 0.039$, 0.01, and 0.024, respectively). Regarding age, no statistically significant difference was found between the healthy group and the asymptomatic group ($P = 0.087$) or the NPC group ($P = 0.155$). A significant difference was found between the healthy group and the symptomatic group ($P < 0.001$). An example PET image from the symptomatic group is presented in Figure 2.

As shown in Table 2, the SUV (mean $\pm$ SD) of the LPR in malignant lesions was significantly higher than that in benign lesions (3.0 ± 1.16) ($P < 0.001$). However, when the ratio of LPR uptake to palatine tonsil uptake (N/P ratio) was measured, a relatively lower ratio was observed in benign lesions (0.81 ± 0.37) than in malignant lesions (2.30 ± 1.62) ($P < 0.001$). In addition, CT showed symmetric ^{18}F-FDG uptake in the LPR in 57 subjects (71%) with benign lesions, whereas only 4 subjects (19%) with malignant lesions showed symmetric uptake. Most (81%) of the lesions in malignant disease exhibited asymmetric

TABLE 1
SUVs of Various Regions of Waldeyer's Ring and Salivary Glands in the Healthy, Asymptomatic, Symptomatic, and NPC Groups

Group	n	Mean age ± SD (y)	SUV						
			Nasopharynx	Palatine tonsil	Lingual tonsil	Soft palate	Parotid gland	Submandibular gland	Sublingual gland
Healthy	30	51.9 ± 9.6							
Mean			1.36	3.22	2.22	2.50	1.13	1.43	2.32
SD			0.28	0.71	0.63	0.45	0.27	0.37	0.87
Asymptomatic	53	48.7 ± 10.9							
Mean			2.90*†	3.97*†	2.58*†	2.74	1.30	1.68*†	2.69
SD			1.02	1.54	0.85	0.75	0.60	0.48	0.90
Symptomatic	27	43.4 ± 9.2							
Mean			3.18*†	3.97*†	2.89*†	2.88	1.33	1.65*†	2.47
SD			1.38	1.58	1.08	2.03	0.49	0.47	0.87
NPC	21	48.1 ± 14.9							
Mean			7.03*	3.31	2.21	2.55	1.23	1.38	2.64
SD			3.83	0.95	0.80	0.75	0.48	0.41	0.95

*Significant difference ($P < 0.05$) compared with healthy group.
†Significant difference ($P < 0.05$) compared with NPC group.
Nasopharynx = LPR of nasopharynx.

uptake. The incidence of wall thickening of the LPR was significantly higher in 17 subjects (81%) with malignant lesions, 16 of whom had asymmetric thickening, than in 15 subjects (18.8%) with benign lesions. The differences between benign and malignant lesions were statistically significant for symmetric/asymmetric ¹⁸F-FDG uptake in the LPR ($P < 0.01$) and for symmetric/asymmetric wall thickening of the LPR ($P < 0.001$). The associated ¹⁸F-FDG uptake in the cervical lymph nodes, which was rare (5%) in subjects with benign lesions, was observed in 19
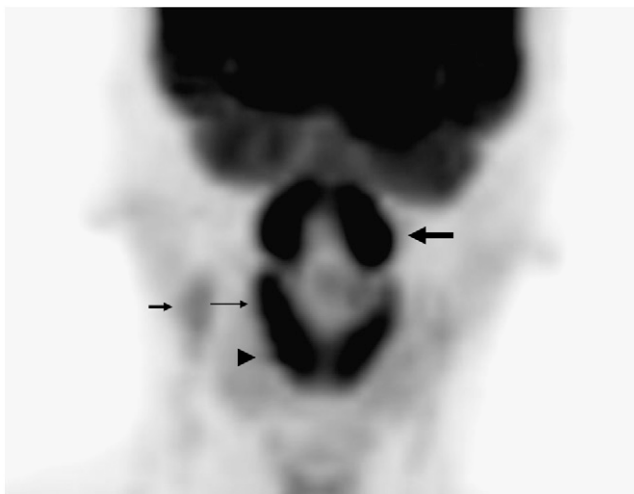
FIGURE 2. Maximum-intensity-projection PET image reveals symmetrically intense ¹⁸F-FDG uptake in LPR (thick long arrow), palatine tonsil (thin long arrow), and lingual tonsil (arrowhead) in 39-y-old man with upper respiratory airway infection. Mild ¹⁸F-FDG uptake in right high jugular lymph nodes (short arrow) is also seen.

subjects (90%) with malignant lesions. Figure 3 shows images of a patient with NPC.

The distribution of SUVs in the LPR for each studied group is shown in Figure 4. Discriminating benign from malignant lesions was difficult because of an overlap of SUVs. When an SUV of 3.9 was used as the cutoff for discriminating benign from malignant lesions, 10 (19%) of the 53 subjects in the asymptomatic group and 7 (26%) of the 27 subjects in the symptomatic group had an SUV exceeding this cutoff level in the LPR. They were regarded as false-positives for malignancy. However, the N/P ratio was relatively lower in the symptomatic group (0.9 ± 0.3) (N = 5.1 ± 0.3, P = 5.9 ± 0.6) than in the asymptomatic group (1.3 ± 0.4) (N = 4.7 ± 0.7, P = 3.8 ± 1.5) ($P = 0.012$), indicating that active infection or inflammation of the palatine tonsils, inducing higher SUVs, might have existed in symptomatic subjects. Five (24%) of the 21 patients with NPC had LPR SUVs of less than 3.9 and had lower N/P ratios (0.8 ± 0.1) (N = 2.4 ± 0.6, P = 3.1 ± 0.7). Among these 5 patients regarded as "false-negatives" for NPC, 4 (80%) also showed symmetric ¹⁸F-FDG uptake in the LPR. However, neck lymph node uptake was detected in all these patients.

When the LPR SUV was used to differentiate benign from malignant lesions on receiver-operating-characteristic curve analysis, the AUC of ¹⁸F-FDG PET was 0.81 ± 0.06 (95% confidence interval [CI], 0.72–0.88), with a sensitivity of 72% and specificity of 80%. When the N/P ratio was used, the AUC was 0.87 ± 0.05 (95% CI, 0.79–0.93), with a sensitivity of 67% and specificity of 95%. The receiver-operating-characteristic curve and AUC showed no statistically significant difference between these 2 parameters

TABLE 2
Comparison of PET/CT Findings in LPR of Nasopharynx, Palatine Tonsil, and Cervical Lymph Nodes Between Benign and Malignant (NPC) Lesions

Finding	Benign (n = 80)	Malignant (n = 21)	P
PET			
SUV (mean ± SD) of LPR	3.0 ± 1.16 (range, 1.2–7.7)	7.03 ± 3.83 (range, 1.9–15.6)	<0.001
N/P ratio (mean ± SD)	0.81 ± 0.37 (range, 0.3–2.1)	2.30 ± 1.62 (range, 0.7–7.3)	<0.001
^{18}F-FDG uptake in LPR			
Symmetric	57 (71%)	4 (19%)	<0.001
Asymmetric	23 (29%)	17 (81%)	
Neck lymph node uptake			
Unilateral	3	3	<0.001
Bilateral	1	16	
Negative	76	2	
CT			
Wall thickening of LPR			
Symmetric	7	1	<0.001
Asymmetric	8	16	
Negative	65	4	

($P = 0.228$). When an SUV of less than 3.9 and an N/P ratio of less than 1.5 were used as the cutoff points in subjects showing the combination of symmetric uptake in the LPR, normal or symmetric wall thickening, and detectable neck lymph node uptake, the AUC of PET/CT was improved significantly to $0.932 ± 0.042$ (95% CI, 0.86–0.98) ($P = 0.005$), with a sensitivity of 90.4% and a specificity of 93.8% (Fig. 5).

DISCUSSION

The nasopharyngeal cavity is the uppermost part of the aerodigestive tract. Anteriorly, it is contiguous with the nasal cavity by way of the posterior choanae. The adenoids, or pharyngeal tonsils, are lymphatic tissues located in the midline roof of the nasopharynx. Tubal tonsils lie around the eustachian tubes. The lingual (floor), pharyngeal (roof), and palatine (lateral wall) tonsils compose the bulk of the so-called Waldeyer's ring of lymphatic tissue that lines the walls of the nasopharynx and oropharynx. Tonsils and adenoids are located near the entrance of the breathing passages, where they can catch incoming germs that cause infections. Normal lymphoid tissue of Waldeyer's ring appears as homogeneous soft tissue that is sometimes lobulated. CT can clearly depict the anatomic locations of the aforementioned structures, whereas PET cannot. However, differentiation between normal lymphoid tissue and inflamed or hypertrophic tissue or a tumor may be difficult.

^{18}F-FDG PET is sensitive for the diagnosis and staging of several types of malignancy. However, ^{18}F-FDG accumulation is not specific to tumors. ^{18}F-FDG uptake in benign processes has numerous causes (9). The increased uptake of ^{18}F-FDG at suspected sites of inflammation and infection is utilized for detecting varieties of inflammatory and infectious disorders (11,12). The increased uptake of ^{18}F-FDG in certain types of unknown benign lesions also gives rise to false-positive results when a patient is being imaged to evaluate a potential malignant disorder. Many studies have found a significant increase in NPC in patients with a previous history of ear, nose, and throat disease (1).

In this study, 4.9% of the subjects had focally increased ^{18}F-FDG uptake in the LPR of the nasopharynx and were finally found to have benign lesions. Among them, two thirds of the subjects were asymptomatic. An associated increase in ^{18}F-FDG uptake in the palatine tonsil, lingual tonsil, or salivary glands was observed, indicating that an infectious or inflammatory process was present in these regions. Distinguishing malignant lesions from benign inflammatory or infectious processes is challenging because both can cause

FIGURE 3. A 49-y-old man with newly diagnosed NPC who underwent PET/CT for staging. (A) CT image shows wall thickening (arrow) of right LPR. (B and C) Only mild ^{18}F-FDG uptake (thick arrows) in right LPR is demonstrated in transaxial (B) and maximum-intensity-projection (C) PET views. In addition, maximum-intensity-projection PET view shows ^{18}F-FDG uptake in palatine tonsil (thin arrow) and neck lymph nodes (short arrows).
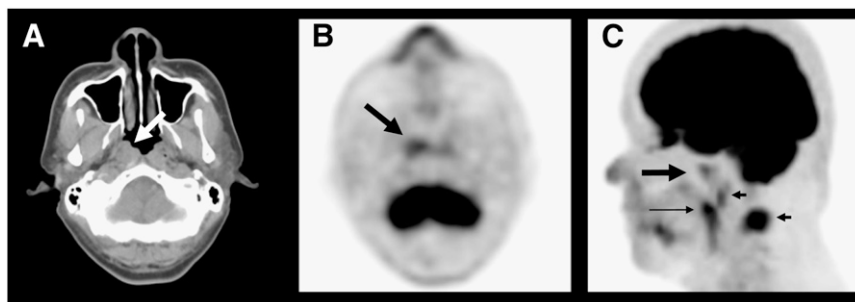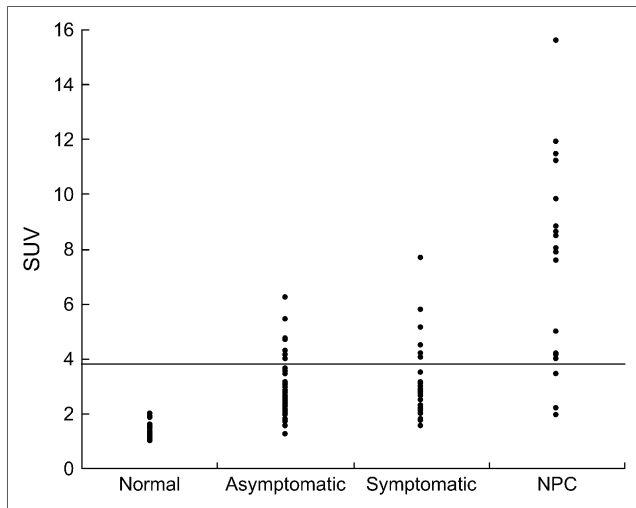
FIGURE 4. Distribution of SUVs in LPR region of healthy, asymptomatic, and symptomatic subjects and patients with NPC.
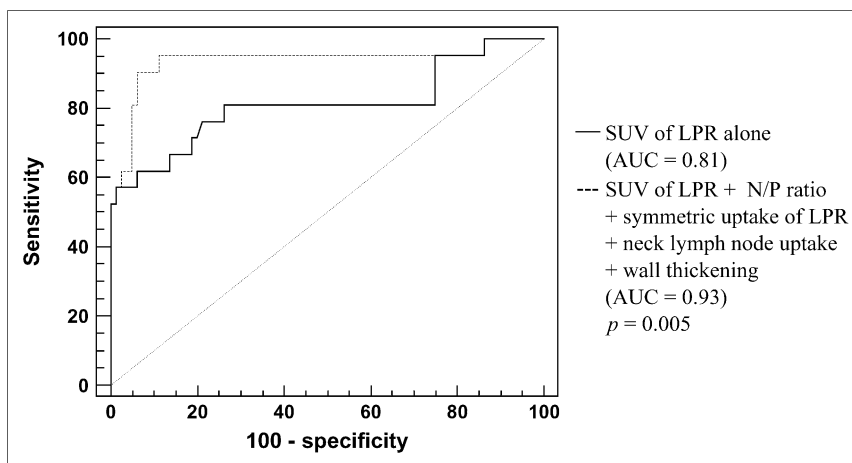
increased ^{18}F-FDG uptake. SUVs have been proposed as being useful for discrimination. The cutoff value is controversial, although 2.5–3.9 is generally accepted. However, considerable overlap still exists between malignant and benign lesions. A dual-phase technique was suggested in an attempt to enhance diagnostic accuracy (*13,14*). However, the results appeared to be disappointing (*15,16*). In this study, an SUV of more than 3.9 was found in 17 (21%) of the 80 subjects with benign lesions, among which 10 subjects (59%) were asymptomatic and 7 (41%) were symptomatic. In contrast, 5 (24%) of the 21 patients with NPC had an SUV of less than 3.9. Therefore, criteria other than the SUV were needed to improve the accuracy of characterizing LPR lesions. Complementary use of the N/P ratio in an attempt to differentiate benign from malignant lesions was also evaluated in this study. Although subjects with benign lesions had lower N/P ratios, the result did not seem to be promising

because no statistical difference was observed when each of these 2 parameters was used alone. Relatively higher ^{18}F-FDG uptake in the palatine tonsil (SUV, 5.9 ± 0.6), resulting in a lower N/P ratio and regarded as false-positive for malignancy, was found exclusively in symptomatic subjects, indicating that subjects presenting with active processes other than chronic inflammation might exhibit more enhanced ^{18}F-FDG metabolism in the palatine tonsil. Hence, clinical evaluations are necessary when acquiring and interpreting the images.

Symmetric or asymmetric uptake and mucosal thickening of the LPR were other parameters considered, because infection and inflammation induce increased tissue activity, and morphologic hypertrophy might occasionally occur bilaterally. These phenomena were observed in most cases of benign lesions in this study. NPC patients usually have bilateral metastases in the neck nodes at presentation. In the literature, 60%–90% of patients have nodal spread at the time of initial diagnosis, and nearly 50%–80% of patients have bilateral disease. The presence of lymph node enlargement has, however, no relationship to the size of the primary tumor (*17–21*). Of the 21 patients with NPC in this study, ^{18}F-FDG uptake in the neck lymph nodes was found in 19 (90%), among whom 16 exhibited bilateral uptake.

CONCLUSION

When an SUV of less than 3.9 and an N/P ratio of less than 1.5 were used as cutoff points in subjects showing the combination of symmetric uptake in the LPR, normal or symmetric wall thickening, and detectable neck lymph node uptake, the AUC of PET/CT was improved significantly to 0.932 ± 0.042, with a sensitivity of 90.4% and a specificity of 93.8%. These results indicate that the intensity and patterns of ^{18}F-FDG uptake in various regions of Waldeyer's ring along with CT scan findings provide a feasible modality to differentiate benign from malignant nasopharyngeal lesions.

— SUV of LPR alone
(AUC = 0.81)

--- SUV of LPR + N/P ratio
+ symmetric uptake of LPR
+ neck lymph node uptake
+ wall thickening
(AUC = 0.93)
$p = 0.005$

FIGURE 5. Receiver-operating-characteristic curve and AUC for differentiating benign from malignant lesions in LPR of nasopharynx. When combination of SUV, LPR of N/P ratio, symmetric uptake of LPR, cervical lymph node uptake, and wall thickening of LPR was considered, AUC improved to 0.932 ± 0.042 (95% CI, 0.86–0.98), with 90.4% sensitivity and 93.8% specificity.

REFERENCES

1. McDermott AL, Dutt SN, Watkinson JC. The aetiology of nasopharyngeal carcinoma. *Clin Otolaryngol Allied Sci.* 2001;26:82–92.

2. Huang DP. Epidemiology of nasopharyngeal carcinoma. *Ear Nose Throat J.* 1990;69:222–225.

3. Vokes EE, Liebowitz DN, Weichselbaum RR. Nasopharyngeal carcinoma. *Lancet.* 1997;350:1087–1091.

4. Makitie AA, Reis PP, Irish J, et al. Correlation of Epstein-Barr virus DNA in cell-free plasma, functional imaging and clinical course in locally advanced nasopharyngeal cancer: a pilot study. *Head Neck.* 2004;26:815–822.

5. Evans AS. Clinical syndromes associated with EB virus infection. *Adv Intern Med.* 1972;18:77–93.

6. Niedobitek G, Agathanggelou A, Herbst H, et al. Epstein-Barr virus (EBV) infection in infectious mononucleosis: virus latency, replication and phenotype of EBV-infected cells. *J Pathol.* 1997;182:151–159.

7. AAssar OS, Fischbein NJ, Caputo GR, et al. Metastatic head and neck cancer: role and usefulness of FDG PET in locating occult primary tumors. *Radiology.* 1999;210:177–181.

8. Nakamoto Y, Tatsumi M, Hammoud D, Cohade C, Osman MM, Wahl RL. Normal FDG distribution patterns in the head and neck: PET/CT evaluation. *Radiology.* 2005;234:879–885.

9. Bakheet SM, Powe J. Benign causes of 18-FDG uptake on whole body imaging. *Semin Nucl Med.* 1998;28:352–358.

10. Chen YK, Su CT, Ding HJ, et al. Clinical usefulness of fused PET/CT compared with PET alone or CT alone in nasopharyngeal carcinoma patients. *Anticancer Res.* 2006;26:1471–1478.

11. Sugawara Y, Braun D, Kison P, Russo J, Zasadny K, Wahl R. Rapid detection of human infections with fluorine-18 fluorodeoxyglucose and positron emission tomography: preliminary results. *Eur J Nucl Med.* 1998;25:1238–1243.

12. Zhuang H, Duarte PS, Pourdehand M, Shnier D, Alavi A. Exclusion of chronic osteomyelitis with F-18 fluorodeoxyglucose positron emission tomographic imaging. *Clin Nucl Med.* 2000;25:281–284.

13. Hubner KF, Buonocore E, Gould HR, et al. Differentiating benign from malignant lung lesions using "quantitative" parameters of FDG PET images. *Clin Nucl Med.* 1996;21:941–949.

14. Zhuang H, Pourdehnad M, Lambright ES, et al. Dual time point ^{18}F-FDG PET imaging for differentiating malignant from inflammatory processes. *J Nucl Med.* 2001;42:1412–1417.

15. Ng SH, Joseph CT, Chan SC, et al. Clinical usefulness of ^{18}F-FDG PET in nasopharyngeal carcinoma patients with questionable MRI findings for recurrence. *J Nucl Med.* 2004;45:1669–1676.

16. Yen TC, Chang YC, Chan SC, et al. Are dual-phase F-18-FDG PET scans necessary in nasopharyngeal carcinoma to assess the primary tumor and locoregional nodes? *Eur J Nucl Med Mol Imaging.* 2005;32:541–548.

17. Ng SH, Chang JT, Chan SC, et al. Nodal metastases of nasopharyngeal carcinoma: patterns of disease on MRI and FDG PET. *Eur J Nucl Med Mol Imaging.* 2004;31:1073–1080.

18. Sun Y, Ma J, Lu TX, Wang Y, Huang Y, Tang LL. Regulation for distribution of metastatic cervical lymph nodes of 512 cases of nasopharyngeal carcinoma. *Ai Zheng.* 2004;23:1523–1527.

19. Yen TC, Chang JT, Ng SH, et al. The value of ^{18}F-FDG PET in the detection of stage M0 carcinoma of the nasopharynx. *J Nucl Med.* 2005;46:405–410.

20. Chang JT, Chan SC, Yen TC, et al. Nasopharyngeal carcinoma staging by ^{18}F-fluorodeoxyglucose positron emission tomography. *Int J Radiat Oncol Biol Phys.* 2005;62:501–507.

21. Yen RF, Hong RL, Tzen KY, Pan MH, Chen TH. Whole-body ^{18}F-FDG PET in recurrent or metastatic nasopharyngeal carcinoma. *J Nucl Med.* 2005;46:770–774.